ORGANOMETALLICS

Article

pubs.acs.org/Organometallics

Reactivity of Ytterbium(II) Hydride. Redox Reactions: Ytterbium(II) vs Hydrido Ligand. Metathesis of the Yb−H Bond

Ivan V. Basalov, Dmitry M. Lyubov, Georgy K. Fukin, Anton V. Cherkasov, and Alexander A. Trifonov*

G. A. Razuvaev Institute of Organometallic Chemistry of Russian Academy of Sciences, Tropinina 49, GSP-445, 603950 Nizhny Novgorod, Russia

Supporting Information

ABSTRACT: Oxidation reactions of the Yb(II) hydride [{*t*BuC(NC$_6$H$_3$-2,6-*i*Pr$_2$)$_2$}Yb(μ-H)]$_2$ (**1**) with CuCl (1:2 molar ratio) and (PhCH$_2$S)$_2$ (1:1 molar ratio) revealed that the hydrido anion in **1** is a stronger reductant than the Yb(II) cation. Both reactions occur with evolution of H$_2$ and afford the dimeric Yb(II) species [{*t*BuC(NC$_6$H$_3$-2,6-*i*Pr$_2$)$_2$}Yb(μ-X)]$_2$ (X = Cl (**2**), SCH$_2$Ph (**3**)) in which a κ^1-amido,η^6-arene type of coordination of amidinate ligand is retained. Reaction of **1** with 2 equiv of (PhCH$_2$S)$_2$ results in oxidation of both Yb(II) and hydrido centers and leads to the formation of the Yb(III) complex [{*t*BuC(NC$_6$H$_3$-2,6-*i*Pr$_2$)$_2$}Yb(μ-SCH$_2$Ph)$_2$]$_2$ (**4**). Complex **4** can be also synthesized by oxidation of **3** with an equimolar amount of (PhCH$_2$S)$_2$. It was demonstrated that oxidation of the ytterbium center to the trivalent state leads to switching of the coordination mode of amidinate ligand from κ^1-amido, η^6-arene to "classical" κ^1,κ^1-N,N-chelating. Unlike Yb(III) bis(alkyl) species supported by bulky amidopyridinate ligands, the reaction of [{*t*BuC(NC$_6$H$_3$-2,6-*i*Pr$_2$)$_2$}Yb(CH$_2$SiMe$_3$)$_2$(THF)] (**6**) with PhSiH$_3$ (1:2 molar ratio) occurs with reduction of ytterbium to a divalent state and affords **1**. Thus, reduction of Yb(III) to Yb(II) leads to a change of coordination mode from κ^1,κ^1-N,N to κ^1-N, η^6-arene. Oxidation of **1** by 2,6-*i*Pr$_2$C$_6$H$_3$N=C(H)C(H)=NC$_6$H$_3$-2,6-*i*Pr$_2$ was found to result in oxidation of the hydrido ligand and ytterbium ion and formation of the mixed-valent ion-pair complex [{*t*BuC(NC$_6$H$_3$-2,6-*i*Pr$_2$)$_2$}Yb(DME)$_2$]$^+$[{2,6-*i*Pr$_2$C$_6$H$_3$NC(H)=C(H)NC$_6$H$_3$-2,6-*i*Pr$_2$}$_2$Yb]$^-$ (**5**). The σ-bond metathesis reaction of **1** with Ph$_2$PH allowed for the synthesis of the first mixed-ligand hydrido−phosphido Yb(II) species [{*t*BuC(NC$_6$H$_3$-2,6-*i*Pr$_2$)$_2$}Yb(μ-H)(μ-PPh$_2$)Yb{*t*BuC(NC$_6$H$_3$-2,6-*i*Pr$_2$)$_2$}] (**7**). The second hydrido ligand cannot be replaced by a phosphido ligand.

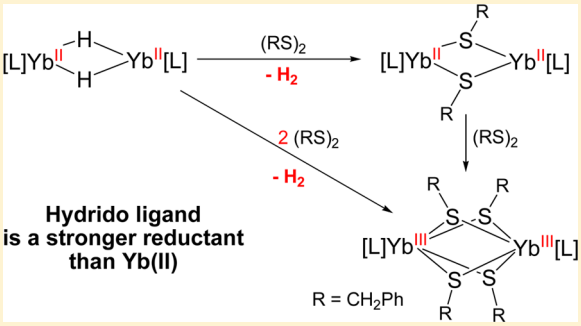

INTRODUCTION

Hydrido complexes belong to the most interesting and promising classes of organolanthanides. Their unique reactivity in stoichiometric reactions[1] and catalytic activity in a variety of olefinic transformations have stimulated intense development of this chemistry.[2] Although the first reports on lanthanide hydrides appeared in the 1980s,[3] hydrido species of lanthanides in a divalent state still remain virtually unexplored.[4] The first structurally defined Ln(II) hydrido complex supported by a bulky hydrotris(pyrazolyl)borate ligand was published by Takats et al. in 1999.[4a] Another example of a Yb(II) hydride involves a complex coordinated by a DIPP-nacnac ligand.[4b] Despite the fact that some classes of stoichiometric reactions of [(Tp^{tBu,Me})Yb(μ-H)]$_2$[4a] and the catalytic activity of [(DIPP-nacnac)YbH(thf)]$_2$[4b] in 1,1-diphenylethylene hydrosilylation[4b] have been described, the reactivity of Ln(II) hydrido species still remains poorly investigated. Indeed, Ln(II) hydrido complexes containing two reaction centers which can provide various types of reactivities present great interest for the investigation of reactivity patterns. The presence of a low-valent Yb(II) ion and hydrido ligand possessing reductive properties gives a basis for a rich redox chemistry of these complexes. Moreover, to date it is not clear which partner in the couple Yb(II)−H$^-$ is a stronger reductant. The Yb−H bond can undergo insertions of multiple bonds as well as σ-bond metathesis reactions with reagents containing acidic X−H bonds. The existence in the same molecule of Lewis acidic (Yb ion) and basic (M−H) sites can lead to rich coordination chemistry. The synthesis of monomeric hydrido species[1b,5] still remains a challenge in organolanthanide chemistry, that is why splitting of a dimeric Ln$_2$H$_2$ core under treatment with Lewis base or acid seems to be an ongoing trend.

Recently we reported on the synthesis, structure, and reactivity of the novel Yb(II) hydrido complex [{*t*BuC(NC$_6$H$_3$-2,6-*i*Pr$_2$)$_2$}Yb(μ-H)]$_2$ (**1**),[4c] supported by a bulky amidinate ligand. Complex **1** features a rather unusual κ^1-amido, η^6-arene type of coordination of amidinate ligand with a surprisingly robust Yb(II)−η^6-arene interaction. We found that despite the highly oxophilic nature of lanthanide metals arene could not be replaced from the metal coordination sphere when **1** was treated with Lewis bases. Moreover, complex **1** exhibited an ability for double addition to a C≡C bond, affording a

Special Issue: Recent Advances in Organo-f-Element Chemistry

Received: January 10, 2013
Published: February 14, 2013

   dx.doi.org/10.1021/om400015k | *Organometallics* 2013, 32, 1507−1516

Scheme 1

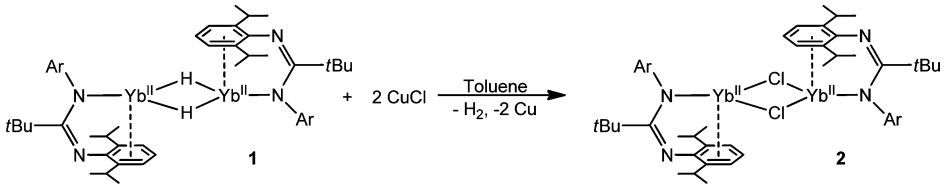

dimeric complex with a 1,2-dianionic bibenzyl ligand. Preliminary studies on the oxidation of **1** revealed that both Yb(II) and hydrido centers are oxidized under the reaction conditions. Herein we report on the selective competitive oxidation of Yb(II) ion and hydrido ligand and metathesis of the Yb−H bond with Ph_2PH.

RESULT AND DISCUSSION

In order to estimate the comparative reductive capacities of the hydrido ligand and Yb(II) ion in our previous work, a series of reactions of **1** with one-electron oxidants (I_2, $AgBF_4$, $AgBPh_4$, *N*,*N*′-dimethylthiuram disulfide) was carried out.[4c] The reactions of **1** with I_2, $AgBF_4$, and $AgBPh_4$ turned out to be not selective and resulted in oxidation of both the Yb(II) ion and hydrido ligand. These reactions lead to hydrogen evolution (resulting from oxidation of the hydrido anion) and the formation of intractable mixtures of products containing both Yb(II) and Yb(III) species.[4c] The reaction with the milder oxidant *N*,*N*′-dimethylthiuram disulfide occurred without H_2 evolution, but regardless of the reagent ratio the bis(dithiocarbamato)amidinato Yb(III) complex $[\{t\text{BuC}(NC_6H_3\text{-}2,6\text{-}i\text{Pr}_2)_2\}\text{Yb}(S_2CNMe_2)_2]$ was isolated from the reaction mixture.

Finally we succeeded in choosing selective one-electron oxidants which allowed us to identify a stronger reductant within the Yb(II)−hydrido anion couple. Thus, the reaction of complex **1** with 2 molar equiv of copper(I) chloride occurs selectively in toluene solution at −60 °C and results in evolution of H_2 along with precipitation of metallic copper. From the reaction mixture the ytterbium(II) chloro complex $[\{t\text{BuC}(NC_6H_3\text{-}2,6\text{-}i\text{Pr}_2)_2\}\text{Yb}(\mu\text{-Cl})]_2$ (**2**) (Scheme 1) was isolated in 84% yield.

Complex **2** was isolated as dark red-brownish moisture- and air-sensitive crystals. **2** is well soluble in THF, moderately soluble in toluene or benzene, and poorly soluble in hexane. According to the NMR spectra and magnetic measurements complex **2** is diamagnetic. This indicates a divalent state of the ytterbium metal in **2**. The ^1H and $^{13}C\{^1H\}$ NMR spectra recorded for **2** in C_6D_6 solution at room temperature exhibit the set of signals expected for an amidinate ligand. The methyl and methyne protons of isopropyl groups appear as two complex multiplets at 1.22−1.37 and 3.19−3.45 ppm, respectively; a singlet at 1.44 ppm is assigned to the protons of the *t*Bu group. The aromatic protons of 2,6-diisopropylphenyl groups give rise to a multiplet at 7.01−7.11 ppm. The presence of signals with characteristic satellites due to coupling to ^{171}Yb attributed to quaternary *t*Bu carbons (41.8 ppm, s, ^{171}Yb satellites $^3J_{YbC}$ = 25.7 Hz) and NCN (171.5 ppm, s, ^{171}Yb satellites $^2J_{YbC}$ = 50.1 Hz, NCN) in the $^{13}C\{^1H\}$ NMR spectrum of **2** gives evidence for the coordination of the amidinate ligand to ytterbium.

Crystals of **2** suitable for X-ray analysis were obtained by slow concentration of a toluene solution at room temperature. The X-ray study established the order of connectivity of the atoms in the molecule; however, the poor quality of the crystals does not allow us to discuss the geometric parameters of **2**. The X-ray study revealed that complex **2** adopts a dimeric structure similar to that observed for the parent hydride **1**. The ytterbium centers are connected by two μ-bridging chloro ligands, and the κ^1-N, η^6-arene coordination mode of amidinate ligands is retained. The molecular structure of **2** is depicted in Figure 1.

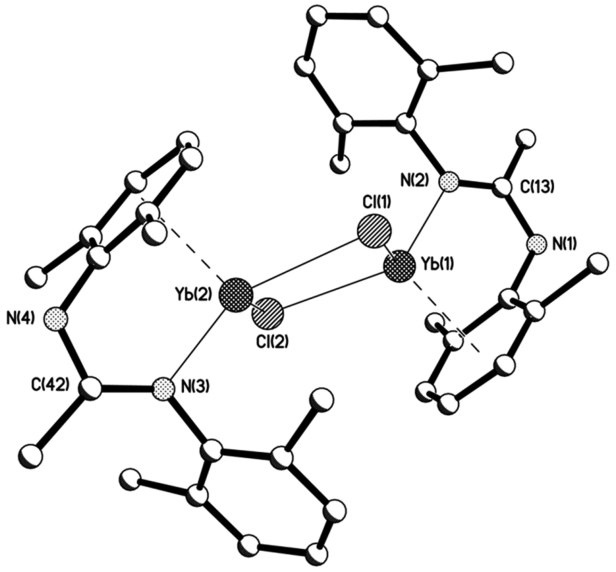

Figure 1. Ball-and-stick plot of $[\{t\text{BuC}(NC_6H_3\text{-}2,6\text{-}i\text{Pr}_2)_2\}\text{Yb}(\mu\text{-Cl})]_2$ (**2**).

Selective oxidation of the hydrido ligand was also performed in the reaction of **1** with an equimolar amount of a mild one-electron oxidant—dibenzyl disulfide $(PhCH_2S)_2$ (toluene, −60 °C). The reaction occurred with H_2 evolution and afforded the related benzyl sulfide Yb(II) complex $[\{t\text{BuC}(NC_6H_3\text{-}2,6\text{-}i\text{Pr}_2)_2\}\text{Yb}(\mu\text{-SCH}_2\text{Ph})]_2$ (**3**), which was isolated in 90% yield (Scheme 2). When the reaction of **1** was carried out with 2 equiv of $(PhCH_2S)_2$ or when **3** was treated with $(PhCH_2S)_2$ (1:1 molar ratio), oxidation of Yb(II) took place; both reactions resulted in the formation of the bis(benzyl sulfide) Yb(III) complex $[\{t\text{BuC}(NC_6H_3\text{-}2,6\text{-}i\text{Pr}_2)_2\}\text{Yb}(\mu\text{-SCH}_2\text{Ph})_2]_2$ (**4**) (Scheme 2). The yields of **4** in these reactions were 92 and 76%, respectively. The magnetic measurements of complex **4** revealed that the value of the effective magnetic moment at room temperature is 4.3 μB, which is indicative of a trivalent oxidation state of the ytterbium atom.[6] Successive oxidation of hydrido and Yb(II) centers in **1** by $(PhCH_2S)_2$ unambiguously demonstrated that in this compound the hydrido ligand is a stronger reductant than the Yb(II) ion.

Complex **3** is well soluble in aromatic solvents and moderately soluble in hexane. According to NMR spectroscopy and magnetic measurements complex **3** is diamagnetic. The ^1H NMR spectrum of **3** in C_6D_6 exhibits a singlet at 0.89 ppm due

dx.doi.org/10.1021/om400015k | *Organometallics* 2013, 32, 1507−1516

Scheme 2

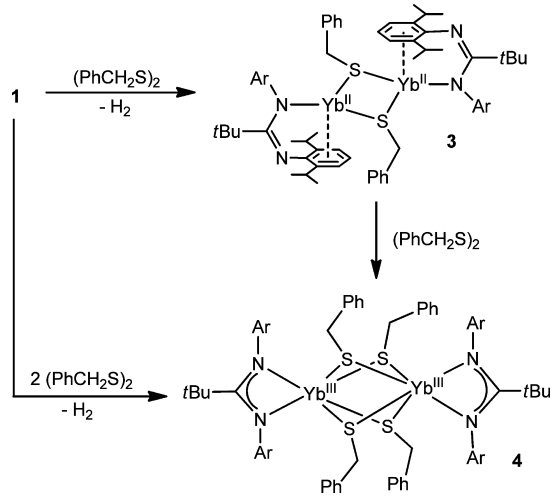

to the protons of the *t*Bu group. The broad singlet at 0.51 ppm and a complex multiplet in the region 1.21−1.34 ppm are assigned to the CH_3 protons of isopropyl groups. The methylene protons of SCH_2Ph fragments along with the methyne protons of isopropyl groups of the amidinate ligand give rise to a complex multiplet in the region 3.04−3.54 ppm. The aromatic protons of $iPr_2C_6H_3$ and SCH_2Ph groups appear in the ^1H NMR spectrum as a multiplet in the region 6.90−7.05 ppm. In the $^{13}C\{^1H\}$ NMR spectrum of **3** the quaternary carbons of NCN and *t*Bu groups exhibit signals with satellites due to coupling to ^{171}Yb (45.7 ppm, s, $^3J_{YbC}$ = 45.1 Hz, CMe_3; 173.9 ppm, s, $^2J_{YbC}$ = 22.5 Hz, NCN).

Single-crystal samples of **3** suitable for X-ray analysis were obtained by slow cooling of a concentrated solution in toluene from 60 °C to room temperature. Complex **3** crystallizes as a toluene solvate. The molecular structure of **3** is depicted in Figure 2; the crystal and structure refinement data are given in Table 1. The X-ray study revealed that **3** adopts a dimeric structure where two $\{tBuC(NC_6H_3\text{-}2,6\text{-}iPr_2)_2\}Yb$ fragments are connected by two μ_2-benzyl sulfide groups. It is noteworthy that the amidinate ligand in **3** retains the κ^1-N, η^6-arene coordination mode similar to that in the parent complex **1**. The Yb−N (2.386(4), 2.408(4) Å) and Yb−$Arene_{Centroid}$ (2.432(5), 2.440(5) Å) distances in **3** are slightly longer than those in **1** (Yb−N = 2.329(3) Å; Yb−$Arene_{Centroid}$ = 2.420(4) Å). This fact obviously reflects the greater steric demand of benzyl sulfide groups in comparison to hydrido ligands. The Yb−S distances in **3** fall into the region 2.7599(12)−2.8116(12) Å, which correspond to the related distances previously reported for the dimeric Yb(II) thiolate complex $[(C_4Me_4P)Yb(\mu\text{-}SPh)(THF)_2]_2$ (Yb−S = 2.789(4)−2.834(4) Å).[7] In complex **3**, unlike in $[(C_4Me_4P)Yb(\mu\text{-}SPh)(THF)_2]_2$, the four-membered Yb_2S_2 core is not planar; the value of the dihedral angle between the planes S(1)−Yb(1)−S(2) and S(1)−Yb(2)−S(2) is 145.8°. The Yb(1)−Yb(2) distance (4.101(4) Å) in **3** is substantially shorter in comparison to that in $[(C_4Me_4P)Yb(\mu\text{-}SPh)(THF)_2]_2$ (4.596(4) [4.669(4)] Å), where the Yb_2S_2 core is planar.

Single-crystal samples of **4** suitable for X-ray analysis were obtained by slow cooling of a concentrated solution in toluene from 60 °C to room temperature. The molecular structure of **4** is depicted in Figure 3; the crystal and structure refinement data are given in Table 1. According to the X-ray study **4** adopts

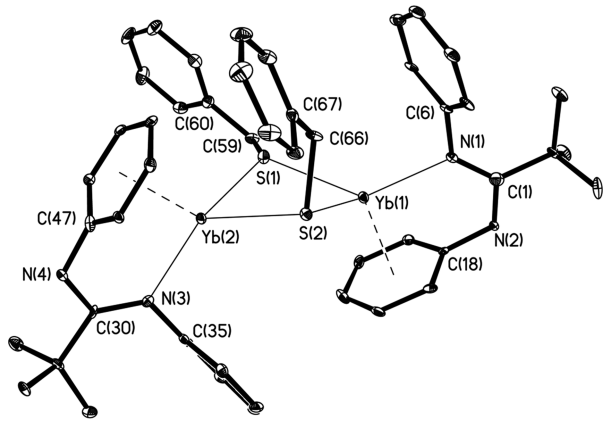

Figure 2. Molecular structure of $[\{tBuC(NC_6H_3\text{-}2,6\text{-}iPr_2)_2\}Yb(\mu\text{-}SCH_2Ph)]_2$ (**3**). Thermal ellipsoids are drawn at the 30% probability level. Hydrogen atoms and isopropyl carbons are omitted for clarity. Selected distances (Å) and angles (deg): Yb(1)−N(1) = 2.386(4), Yb(1)−S(1) = 2.7599(12), Yb(1)−S(2) = 2.7694(12), Yb(2)−N(3) = 2.408(4), Yb(2)−S(1) = 2.7622(13), Yb(2)−S(2) = 2.8116(12), Yb(1)−C_{Arene} = 2.723(5)−2.862(5), Yb(1)−$Arene_{Centroid}$ = 2.432, Yb(2)−C_{Arene} = 2.729(5)−2.853(5), Yb(2)−$Arene_{Centroid}$ = 2.440, Yb(1)−Yb(2) = 4.101(4); Yb(1)−S(1)−Yb(2) = 95.91(4), Yb(1)−S(2)−Yb(2) = 94.57(4), S(1)−Yb(1)−S(2) = 79.13(4), S(1)−Yb(2)−S(2) = 78.38(4), N(1)−C(1)−N(2) = 120.6(4), N(3)−C(30)−N(4) = 121.8(4), $Arene_{Centroid}$−Yb(1)−N(1) = 91.9, $Arene_{Centroid}$−Yb(2)−N(3) = 91.5.

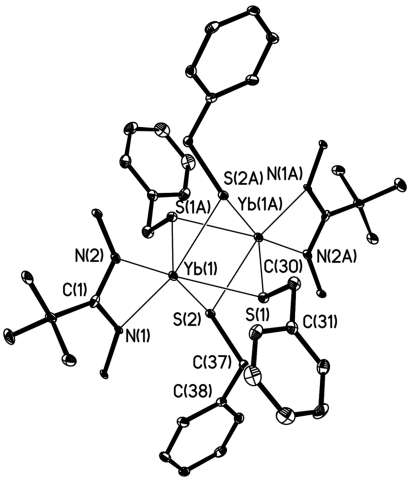

Figure 3. Molecular structure of $[\{tBuC(NC_6H_3\text{-}2,6\text{-}iPr_2)_2\}Yb(\mu\text{-}SCH_2Ph)_2]_2$ (**4**). Thermal ellipsoids are drawn at the 30% probability level. Symmetry transformations used to generate equivalent A atoms: *−x, −y, −z* + 1. Hydrogen atoms and 2,6-$iPr_2C_6H_3$-groups are omitted for clarity. Selected distances (Å) and angles (deg): Yb(1)−N(1) = 2.291(3), Yb(1)−N(2) = 2.294(3), Yb(1)−S(1) = 2.6998(11), Yb(1)−S(1a) = 2.7603(10), Yb(1)−S(2) = 2.7716(9), Yb(1)−S(2a) = 2.7877(9), Yb(1)−Yb(1a) = 3.2862(4), N(1)−C(1) = 1.349(4), N(2)−C(1) = 1.341(5); N(1)−Yb(1)−N(2) = 57.17(11), S(1)−Yb(1)−S(1a) = 106.01(3), S(2)−Yb(1)−S(2a) = 107.53(2), S(1)−Yb(1)−S(2) = 68.65(3), N(1)−C(1)−N(2) = 109.2(3).

a dimeric structure where two $\{tBuC(NC_6H_3\text{-}2,6\text{-}iPr_2)_2\}Yb$ moieties are linked by four μ_2-benzyl sulfide fragments. The most important structural feature of **4** is the coordination mode of the amidinate ligand. In contrast to the κ^1-N, η^6-arene coordination mode detected in Yb(II) species **1**−**3**, oxidation of the ytterbium center to a trivalent state leads to switching to the "classical" κ^1,κ^1-N,N-chelating mode characteristic of Ln(III)

dx.doi.org/10.1021/om400015k | *Organometallics* 2013, 32, 1507−1516

Scheme 3

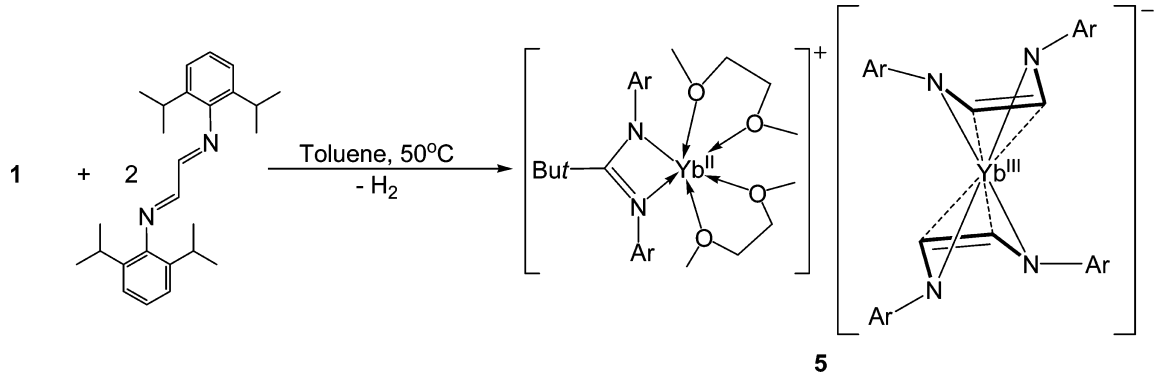

amidinates.[8] The Yb−N (2.291(3), 2.294(3) Å) and C−N (1.349(4), 1.341(5) Å) bonds within the YbNCN fragment are equivalent, indicating a symmetric coordination to the metal ion with delocalization of the negative charge within the conjugated amidinate ligand. The Yb−N distances in **4** are slightly shorter in comparison to the related values measured for six-coordinated amidinate Yb(III) compounds (2.290(4)−2.385(4) Å).[9] Formerly it was shown that κ^1-N, η^6-arene coordination of amidinate and guanidinate ligands bearing bulky aryl groups by nitrogen atoms is characteristic of Yb(II) derivatives,[4c,10] and the interconversion of κ^1-N, η^6-arene and κ^1,κ^1-N,N coordination modes can be driven by modification of steric and coordination saturation of the metal. Herein we have demonstrated that a change of oxidation state of Yb(II) to Yb(III) leads to switching of the coordination mode of amidinate ligand from κ^1-N, η^6-arene to κ^1,κ^1-N,N. This can originate from a decrease of ytterbium ion size caused by its oxidation from Yb(II) to Yb(III)[11] as well as from a change of electronic structure of the Yb ion. The fore-membered cores Yb(1)S(1)(S1a)Yb(1a) and Yb(1)S(2)S(2a)Yb(1a) in **4** are planar and adopt a nearly orthogonal orientation (the dihedral angle between the Yb(1)S(1)(S1a)Yb(1a) and Yb(1)S(2)S-(2a)Yb(1a) planes is 88.8°). Due to the difference in ionic radii of Yb(II) and Yb(III) ions in **3** and **4**, the Yb−S and Yb−Yb distances in Yb(III) complex **4** (Yb−S = 2.6998(11)−2.7877(9) Å; Yb−Yb = 3.2862(4) Å) are shorter in comparison to the related distances in the Yb(II) complex **3** (Yb−S = 2.7599(12)−2.8116(12) Å; Yb−Yb = 4.101(4) Å).

Disubstituted 1,4-diazabutadienes established a reputation of mild one- and two-electron oxidants in organolanthanide chemistry capable of oxidizing Yb(II) to Yb(III).[12] This prompted us to attempt oxidation of the Yb(II) hydrido complex **1** with [2,6-iPr$_2$C$_6$H$_3$N═C(H)C(H)═NC$_6$H$_3$-2,6-iPr$_2$] (DAD). One should mention that the reactivity of diazabutadienes toward lanthanide hydrides remains unexplored. In the case of the Yb(II) hydrido complex one can conjecture two reaction pathways. The first pathway is oxidation of the hydrido ligand or of Yb(II), and the second is addition of the Yb−H bond to the C═N bonds of 1,4-diazabutadiene.

The reaction of complex **1** with 2 equiv of DAD was carried out in toluene solution. At 20 °C no reaction was detected in ∼24 h; the starting compounds were recovered from the reaction mixture. At 50 °C the reaction took place. Removal of the solvent under vacuum, treatment of the solid residue with DME, and further recrystallization of the reaction products from a THF/benzene/hexane (1/1/1) mixture allowed the isolation of the mixed-valent ion-pair complex [{tBuC(NC$_6$H$_3$-2,6-iPr$_2$)$_2$}Yb(DME)$_2$]$^+$[{2,6-iPr$_2$C$_6$H$_3$NC(H)═C(H)NC$_6$H$_3$-2,6-iPr$_2$}$_2$Yb]$^-$ (**5**) (Scheme 3), as shown by X-ray crystallography, as brownish green crystals in 23% yield.

Compound **5** crystallizes as the solvate **5**·0.167C$_6$H$_6$·0.167C$_6$H$_{14}$·0.167C$_4$H$_8$O. The asymmetric unit of **5** contains three crystallographically independent molecules. The molecular structures of the cationic and anionic parts of **5** are depicted in Figures 4 and 5 respectively; the crystal and

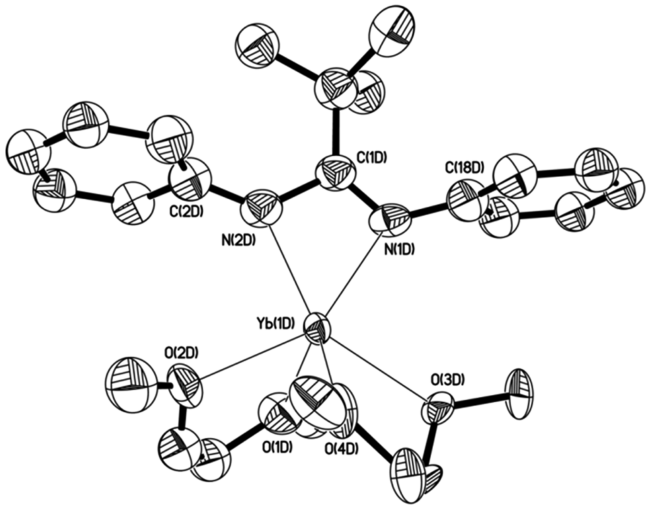

Figure 4. Molecular structure of the cationic part of [{tBuC(NC$_6$H$_3$-2,6-iPr$_2$)$_2$}Yb(DME)$_2$]$^+$[{2,6-iPr$_2$C$_6$H$_3$NC(H)═C(H)NC$_6$H$_3$-2,6-iPr$_2$}$_2$Yb]$^-$ (**5**). Thermal ellipsoids are drawn at the 30% probability level. Hydrogen atoms and isopropyl carbons are omitted for clarity. Selected distances (Å) and angles (deg): Yb(1D)−N(2D) = 2.349(10), Yb(1D)−N(1D) = 2.417(11), Yb(1D)−O(1D) = 2.406(9), Yb(1D)−O(2D) = 2.450(11), Yb(1D)−O(3D) = 2.468(8), Yb(1D)−O(4D) = 2.526(9), N(1D)−C(1D) = 1.268(16), N(2D)−C(1D) = 1.47(2); N(1D)−Yb(1D)−N(2D) = 57.0(4), O(1D)−Yb(1D)−O(2D) = 68.5(3), O(3D)−Yb(1D)−O(4D) = 67.6(3), N(1D)−C(1D)−N(2D) = 112.1(12).

structure refinement data are given in Table 1. The cationic part of **5** consists of a Yb(II) ion coordinated by one monoanionic amidinate ligand and two DME molecules. The coordination mode of the amidinato ligand is κ^1,κ^1-N,N, similar to that previously reported for the Yb(II) amidinate complexes [{tBuC(NC$_6$H$_3$-2,6-iPr$_2$)$_2$}Yb{N(SiMe$_3$)$_2$}(THF)] and [{tBuC(NC$_6$H$_3$-2,6-iPr$_2$)$_2$}$_2$Yb].[4c] The main structural distinction of the cationic part of **5** is a rather unsymmetrical

dx.doi.org/10.1021/om400015k | Organometallics 2013, 32, 1507−1516

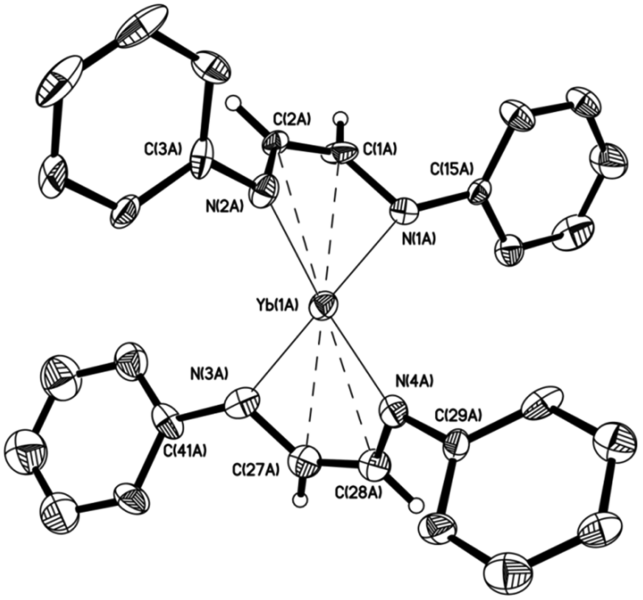

Figure 5. Molecular structure of the anionic part of $[\{t\text{BuC}(NC_6H_3\text{-}2,6\text{-}i\text{Pr}_2)_2\}\text{Yb}(\text{DME})_2]^+[\{2,6\text{-}i\text{Pr}_2C_6H_3\text{NC}(\text{H})\text{=C}(\text{H})\text{NC}_6H_3\text{-}2,6\text{-}i\text{Pr}_2\}_2\text{Yb}]^-$ (**5**). Thermal ellipsoids are drawn at the 30% probability level. Hydrogen atoms of diisopropylphenyl fragments and isopropyl carbons are omitted for clarity. Selected distances (Å) and angles (deg): Yb(1A)−N(1A) = 2.197(8), Yb(1A)−N(2A) = 2.232(7), Yb(1A)−N(3A) = 2.188(7), Yb(1A)−N(4A) = 2.174(9), Yb(1A)−C(1A) = 2.669(10), Yb(1A)−C(2A) = 2.672(8), Yb(1A)−C(27A) = 2.684(9), Yb(1A)−C(28A) = 2.635(10), N(1A)−C(1A) = 1.412(12), N(2A)−C(2A) = 1.440(14), N(3A)−C(27A) = 1.390(12), N(4A)−C(28A) = 1.447(12), C(1A)−C(2A) = 1.337(15), C(27A)−C(28A) = 1.363(15); N(1A)−Yb(1A)−N(2A) = 83.8(3), N(4A)−Yb(1A)−N(3A) = 86.1(3).

coordination mode of the amidinate ligand. Thus, one Yb−N bond (2.349(10) Å) is noticeably shorter in comparison to the second bond (2.417(11) Å). For comparison the Yb−N bond distances in related amidinate Yb(II) complexes are as follows: $[\{t\text{BuC}(NC_6H_3\text{-}2,6\text{-}i\text{Pr}_2)_2\}\text{Yb}\{\text{N}(\text{SiMe}_3)_2\}(\text{THF})]$, 2.377(3) and 2.378(3) Å; $[\{t\text{BuC}(NC_6H_3\text{-}2,6\text{-}i\text{Pr}_2)_2\}_2\text{Yb}]$, 2.363(4)−2.398(4) Å. Nevertheless, the Yb−N distances in the cationic part of **5** give evidence for the divalent state of the ytterbium atom. On the other hand, the bonding situation within the NCN fragment in **5** is rather unusual for an amidinate ligand. The length of one of C−N bond (1.268(16) Å) is indicative of its double-bond character, while the second bond is much longer (1.47(2) Å) and can be considered as a single bond.[13] Thereby no negative charge delocalization takes place in the NCN fragment and it can be classified as an amido-imino ligand.

The anionic part of **5** contains an Yb(III) ion coordinated by two dianionic diazabutadiene ligands. The Yb−N bond distances (2.174(9)−2.232(7) Å) are comparable with the related distances found in the Yb(III) complexes with dianionic enediamido ligands $[\{2,6\text{-}i\text{Pr}_2C_6H_3\text{NC}(\text{H})\text{=C}(\text{H})\text{NC}_6H_3\text{-}2,6\text{-}i\text{Pr}_2\}\text{Yb}(\mu\text{-Cl})(\text{THF})_2]_2$ (2.235(5), 2.209(5) Å)[14] and $[(C_5Me_4R)\text{Yb}\{2,6\text{-}i\text{Pr}_2C_6H_3\text{NC}(\text{R})\text{=C}(\text{R})\text{NC}_6H_3\text{-}2,6\text{-}i\text{Pr}_2\}]$ (R = Me, 2.136(3) and 2.145(3) Å; R = H, 2.141(4) and 2.148(3) Å)[15] and are indicative of the trivalent state of ytterbium. The dianionic diazabutadiene ligands are coordinated to ytterbium in an η^4 fashion. Along with two covalent Yb−N bonds (2.174(9)−2.232(7) Å),[16] short Yb−C contacts (2.635(10)−2.684(9) Å) are also found in **5**. The geometry of the planar NCCN fragments (deviation from the plane −0.028 Å) in **5** is consistent with the dianionic character of the diazabutadiene ligand. The N−C bonds in the diazabutadiene dianion of **5** (1.412(12), 1.440(14) Å and 1.390(12), 1.447(12) Å) are substantially elongated, whereas the C−C bonds (1.337(15) and 1.363(15) Å) are shortened, relative to the N=C (1.266(3) Å) and C−C bond lengths (1.467(5) Å) in the free diazabutadiene molecule.[17] The C−C bond lengths are close to the values of C=C double-bond lengths.[13] The C=C bond of the doubly reduced ene-diamido moiety NCCN also participates in metal−ligand bonding. η^2 coordination of the ene-diamido moiety to the Yb atom results in short Yb−C contacts (2.669(10), 2.672(8) Å and 2.684(9), 2.635(10) Å).

Unfortunately our attempts to isolate other reaction products failed. The formation of **5** obviously results from the oxidation of both hydride and Yb(II) ions and a ligand redistribution reaction.

Recently we reported on the synthesis, structure, and reactivity of trinuclear alkyl hydrido and cationic hydrido clusters supported by bulky amidopyridinate ligands (Ap*) which turned out to be efficient catalysts for ethylene polymerization.[18] We found that the reaction of $[\text{Ap*Yb}(\text{CH}_2\text{SiMe}_3)_2(\text{THF})]$ with 2 equiv of PhSiH_3 afforded $[(\text{Ap*Yb})_3(\mu^2\text{-H})_3(\mu^3\text{-H})_2(\text{CH}_2\text{SiMe}_3)(\text{THF})_2]$.[18a] In order to enlarge the series of alkyl hydrido or polyhydrido clusters, we attempted the reaction of the ytterbium(III) bis(alkyl) complex supported by a bulky amidinate ligand $[\{t\text{BuC}(NC_6H_3\text{-}2,6\text{-}i\text{Pr}_2)_2\}\text{Yb}(\text{CH}_2\text{SiMe}_3)_2(\text{THF})]$ (**6**) with PhSiH_3 (1:2 molar ratio). Complex **6** was prepared by the reaction of $[(\text{Me}_3\text{SiCH}_2)_3\text{Yb}(\text{THF})_2]$ with the amidine $[t\text{BuC}(\text{NHC}_6H_3\text{-}2,6\text{-}i\text{Pr}_2)(NC_6H_3\text{-}2,6\text{-}i\text{Pr}_2)]$ in THF at 0 °C and was isolated in 76% yield (Scheme 4).

Bis(alkyl) complex **6** is extremely air and moisture sensitive but can be stored under vacuum in a crystalline state or in solution for several weeks without any traces of decomposition. **6** is well soluble in toluene and THF and moderately soluble in hexane. The X-ray crystal study revealed that complex **6** is monomeric. The molecular structure of **6** is depicted in Figure

Scheme 4

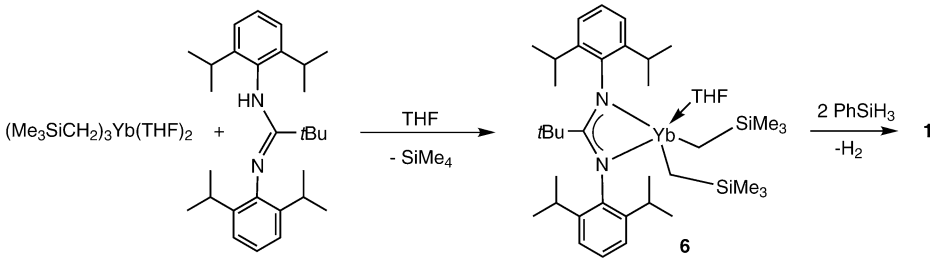

dx.doi.org/10.1021/om400015k | Organometallics 2013, 32, 1507−1516

6; the crystal and structure refinement data are given in Table 1. The coordination environment of the ytterbium atom is made

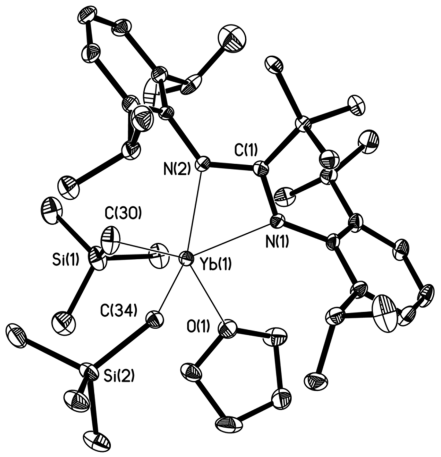

Figure 6. Molecular structure of $[\{t\text{BuC}(\text{NC}_6\text{H}_3\text{-}2,6\text{-}i\text{Pr}_2)_2\}\text{Yb}(\text{CH}_2\text{SiMe}_3)_2(\text{THF})]$ (**6**). Thermal ellipsoids are drawn at the 30% probability level. Hydrogen atoms are omitted for clarity. Selected distances (Å) and angles (deg): Yb(1)−N(1) = 2.3145(19), Yb(1)−N(2) = 2.3295(19), Yb(1)−C(30) = 2.331(3), Yb(1)−C(34) = 2.332(2), Yb(1)−O(1) = 2.3134(17), N(1)−C(1) = 1.345(3), N(2)−C(1) = 1.333(3); N(1)−Yb(1)−N(2) = 56.45(7), C(30)−Yb(1)−C(34) = 108.53(10), N(2)−C(1)−N(1) = 110.2(2).

up of two nitrogen atoms of the chelating amidinato ligand, by two carbon atoms of alkyl groups, and by the oxygen atom of the coordinated THF molecule. The amidinate ligand in **6** is coordinated to the ytterbium atom in a κ^1,κ^1-N,N fashion common for lanthanide(III) complexes. The Yb−N bonds have similar values (2.3145(19), 2.3295(19) Å), reflecting the symmetric coordination of the amidinate ligand. The C−N bond lengths (1.345(3), 1.333(3) Å) within the NCN fragment are equivalent. The Yb−C bond lengths in **6** (2.331(3) and 2.332(2) Å) are very close to the values in previously reported Yb(III) bis(alkyl) species $[(\text{C}_5\text{Me}_4\text{SiMe}_3)\text{Yb}(\text{CH}_2\text{SiMe}_3)_2(\text{THF})]$ (2.336(4), 2.345(4) Å),[19a] $[\{2\text{-}(2,6\text{-}\text{Me}_2\text{C}_6\text{H}_3\text{N})\text{-}\text{C}_6\text{H}_4\text{PPh}_2\}\text{Yb}(\text{CH}_2\text{SiMe}_3)_2(\text{THF})]$ (2.357(3), 2.328(3) Å),[19b] and $[(\text{Tp}^{\text{Me2}})\text{Yb}(\text{CH}_2\text{SiMe}_3)_2(\text{THF})]$ (2.373(2), 2.377(2) Å).[19c]

To our great surprise we found that, unlike $[\text{Ap*Yb}(\text{CH}_2\text{SiMe}_3)_2(\text{THF})]$, the reaction of **6** with 2 equiv of PhSiH_3 (toluene, 0 °C) does not afford the desired Yb(III) polyhydrido cluster supported by an amidinate ligand but occurs with reduction of the ytterbium atom to a divalent state and evolution of H_2, resulting in the formation of complex **1** (Scheme 4). Complex **1** was isolated in 84% yield. Formation of **1** can only be rationalized by the intramolecular reduction of the Yb(III) ion by hydrido ligand to Yb(II).[20] The reaction of equimolar amounts of **6** and PhSiH_3 under similar conditions does not allow for the synthesis of an alkyl hydrido Yb(III) complex coordinated by an amidinate ligand but results in a mixture of starting bis(alkyl) complex **6** and Yb(II) hydride **1**, which were isolated in 35 and 40% yields, respectively.

To date only three Yb(III) polyhydrido complexes supported by bulky amidopyridinate $([(\text{Ap*Yb})_3(\mu_2\text{-H})_3(\mu_3\text{-H})_2(\text{CH}_2\text{SiMe}_3)(\text{THF})_2]$[18b]) or tris(pyrazolyl)borate ligands $([(\text{Tp}^{\text{H2}})\text{Yb}(\mu\text{-H})_2]_6$,[21] $[(\text{Tp}^{\text{Me2}})\text{Yb}(\mu\text{-H})_2]_4$[21]) are known. Among these complexes only the last one demonstrated a tendency to undergo a reductive ligand redistribution reaction which affords Yb(II) species $[(\text{Tp}^{\text{Me2}})_2\text{Yb}]$. Thus, one can conclude that the balance of redox properties in the couple Yb(III/II)−hydrido ligand is very subtle and can be influenced by the ancillary ligand environment.

In order to evaluate the basicity/acidity of the Yb(II)−H bond, the reaction of **1** with an equimolar amount of Ph_2PH was carried out.[22] The reaction occurs in toluene solution at 0 °C with H_2 evolution and formation of a dimeric complex in which only one hydrogen ligand is substituted by phosphido group, $[\{t\text{BuC}(\text{NC}_6\text{H}_3\text{-}2,6\text{-}i\text{Pr}_2)_2\}\text{Yb}(\mu\text{-H})(\mu\text{-PPh}_2)\text{Yb}\{t\text{BuC}(\text{NC}_6\text{H}_3\text{-}2,6\text{-}i\text{Pr}_2)_2\}]$ (**7**) (Scheme 5). Complex **7** does not react with another 1 equiv of Ph_2PH, even at 50 °C.

Scheme 5

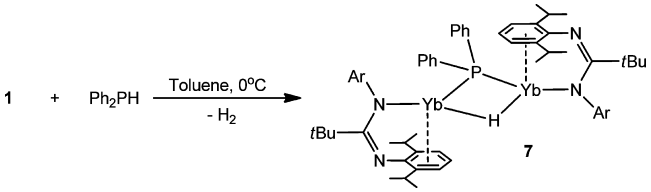

Complex **7** is well soluble in aromatics and moderately soluble in hexane. The single-crystal samples of **7** suitable for X-ray analysis were obtained by slow concentration of a hexane solution at room temperature. The molecular structure of **7** is depicted in Figure 7; the crystal and structure refinement data

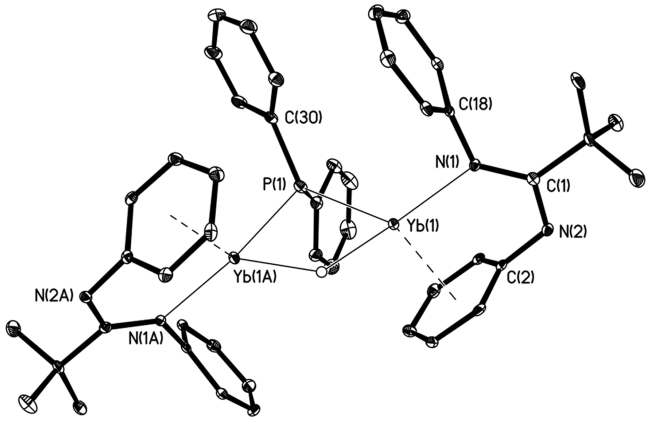

Figure 7. Molecular structure of $[\{t\text{BuC}(\text{NC}_6\text{H}_3\text{-}2,6\text{-}i\text{Pr}_2)_2\}\text{Yb}(\mu\text{-H})(\mu\text{-PPh}_2)\text{Yb}\{t\text{BuC}(\text{NC}_6\text{H}_3\text{-}2,6\text{-}i\text{Pr}_2)_2\}]$ (**7**). Thermal ellipsoids are drawn at the 30% probability level. Symmetry transformations used to generate equivalent A atoms: −x, y, $-z + {}^3/_2$. Hydrogen atoms of amidinate and diphenylphosphine ligand and isopropyl carbons are omitted for clarity. Selected distances (Å) and angles (deg): Yb(1)−N(1) = 2.3838(19), Yb(1)−P(1) = 2.8981(7), Yb(1)−H(1) = 2.22(4), Yb(1)−Yb(1A) = 3.7695(2), Yb(1)−C_{Arene} = 2.709(2)−2.874(3), Yb(1)−$\text{Arene}_{\text{Centroid}}$ = 2.438, N(1)−C(1) = 1.358(3), N(2)−C(1) = 1.316(3); Yb(1)−P(1)−Yb(1A) = 81.13(3), Yb(1)−H(1)−Yb(1A) = 116.5(4), P(1)−Yb(1)−H(1) = 81.2(4), N(2)−C(1)−N(1) = 120.1(2), $\text{Arene}_{\text{Centroid}}$−Yb(1)−N(1) = 92.7.

are given in Table 1. According to the X-ray analysis complex **7** is dimeric, where two $\{t\text{BuC}(\text{NC}_6\text{H}_3\text{-}2,6\text{-}i\text{Pr}_2)_2\}\text{Yb}$ moieties are linked by one μ-hydrido and one μ-diphenylphosphido ligand. The four-membered fragment Yb−H−Yb−P is planar, similar to that in the parent hydrido complex **1**. The Yb−Yb distance in **7** is 3.7695(2) Å and is expectedly longer in comparison to that in **1** (3.3553(4) Å). The bulkier μ-diphenylphosphido ligand affects a reciprocal orientation of the $\{t\text{BuC}(\text{NC}_6\text{H}_3\text{-}2,6\text{-}$

dx.doi.org/10.1021/om400015k | Organometallics 2013, 32, 1507−1516

iPr$_2$)$_2$}Yb fragments. Thus, in **1** the η^6-coordinated aromatic rings are coplanar and two {tBuC(NC$_6$H$_3$-2,6-iPr$_2$)$_2$}Yb are oriented *trans* relative to the Yb$_2$H$_2$ core, while in **7** the value of the dihedral angle between the planes of the η^6-coordinated aromatic rings is 32.3°. The Yb−P bond lengths in **7** (2.8981(7) Å) are comparable with the values previously published for Yb(II) phosphido complexes: [{Me$_2$Si(C$_5$Me$_4$)-(PC$_6$H$_2$-2,4,6-tBu$_3$)}Yb(THF)$_3$] (2.851(4) Å),[23a] [Yb{(μ-PtBu$_2$)$_2$Li(THF)$_2$}$_2$] (2.948(1)−2.985(1) Å).[23b]

In the ^{1}H NMR spectrum of **7** recorded in benzene-d_6 at 293 K the hydrido ligand appears as a doublet at 8.25 ppm due to coupling with ^{31}P nuclei (d, $^2J_{PH}$ = 52 Hz) (Figure 8). This

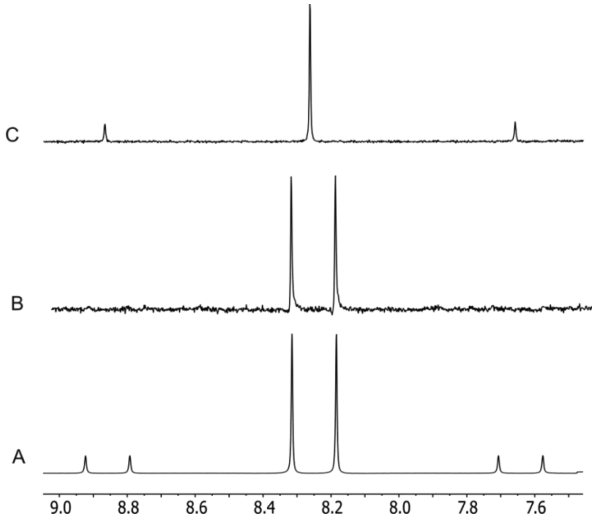

Figure 8. (A) ^{1}H NMR spectrum of **7** (C$_6$D$_6$, 293 K), (B) ^{1}H{^{171}Yb} NMR spectrum of **7** (C$_6$D$_6$, 293 K), and (C) ^{1}H{^{31}P} NMR spectrum of **7** (C$_6$D$_6$, 293 K).

signal also has characteristic satellites reflected in the coupling of the hydrido ligand with ^{171}Yb nuclei ($^1J_{YbH}$ = 486 Hz) (compare the following: **1**, $^1J_{YbH}$ = 460 Hz;[4c] [(Tp^{tBu,Me})YbH]$_2$, $^1J_{YbH}$ = 369 Hz;[4a] [(DIPPnacnac)YbH(THF)]$_2$, $^1J_{YbH}$ = 398 Hz[4b]). The chemical shift of the signal for the hydrido ligand for **7** is shifted to low field in comparison to that for **1** (7.74 ppm)[4c] but shifted upfield in comparison to those for the related Yb(II) hydrides in an N,N-coordination environment: [{(Tp^{tBu,Me})YbH}$_2$] (10.5 ppm)[4a] and [{(DIPPnacnac) YbH-(THF)}$_2$] (9.92 ppm).[4b] The ^{1}H NMR spectrum of **7** gives evidence that a dimeric structure is retained in benzene-d_6 solution (Figure 8). The ^{31}P{^{1}H} NMR spectrum of **7** presents a singlet at 30.9 ppm with satellites due to coupling to ^{171}Yb ($^1J_{YbP}$ = 810 Hz),[24] while in the ^{171}Yb{^{1}H} NMR spectrum a doublet at 1149 ppm (d, $^1J_{YbP}$ = 810 Hz) is observed.[25]

Surprisingly, complex **1** does not react with ^{t}BuC≡CH in toluene, even at 50 °C (72 h).

CONCLUSIONS

CuCl and (PhCH$_2$S)$_2$ turned out to be reagents which allow for selective competitive oxidation of one of two redox-active centers in the Yb(II) hydride [{tBuC(NC$_6$H$_3$-2,6-iPr$_2$)$_2$}Yb(μ-H)]$_2$. Our studies on the oxidation of **1** with CuCl and (PhCH$_2$S) (1:1 molar ratio) elucidated that the hydrido anion in **1** is a stronger reductant than Yb(II). The reactions result in evolution of H$_2$ and afford the dimeric Yb(II) species [{tBuC(NC$_6$H$_3$-2,6-iPr$_2$)$_2$}Yb(μ-X)]$_2$ (X = Cl (**2**), SCH$_2$Ph (**3**)). Reaction of **1** with 2 equiv of (PhCH$_2$S)$_2$ leads to oxidation of both Yb(II) and hydrido centers and the formation of the Yb(III) complex [{[tBuC(NC$_6$H$_3$-2,6-iPr$_2$)$_2$]Yb(μ-SCH$_2$Ph)$_2$}$_2$] (**4**). Complex **4** can be also synthesized by oxidation of **3** with an equimolar amount of (SCH$_2$Ph)$_2$. We found that the κ^1-amido, η^6-arene coordination mode of the amidinate ligand is typical only for Yb(II) species, while oxidation of the metal center results in switching to "classical" κ^1,κ^1-N,N-chelating coordination. Comparison of the results of the reactions of [LYb(CH$_2$SiMe$_3$)$_2$(THF)] (L = Ap*, {tBuC-(NC$_6$H$_3$-2,6-iPr$_2$)$_2$}) with PhSiH$_3$ (1:2 molar ratio) drove us to a conclusion that the balance of reductive properties in the Yb(II/III)−hydrido anion couple is flexible and can be influenced by tuning the nature of the ancillary ligand bound to ytterbium. Reaction of **1** with [2,6-iPr$_2$C$_6$H$_3$N=C(H)C-(H)=NC$_6$H$_3$-2,6-iPr$_2$] was found to result in oxidation of the hydrido ligand and ytterbium ion and to afford the mixed-valent ion-pair complex [{tBuC(NC$_6$H$_3$-2,6-iPr$_2$)$_2$}Yb(DME)$_2$]$^+$[{2,6-iPr$_2$C$_6$H$_3$NC(H)=C(H)NC$_6$H$_3$-2,6-iPr$_2$}$_2$Yb]$^-$ (**5**). It was found that the σ-bond metathesis reaction of **1** with Ph$_2$PH, regardless of the reagent ratio, occurs via substitution of one hydrido ligand. The reaction afforded the first mixed-ligand hydrido phosphido Yb(II) species, [{tBuC(NC$_6$H$_3$-2,6-iPr$_2$)$_2$}-Yb(μ-H)(μ-PPh$_2$)Yb{tBuC(NC$_6$H$_3$-2,6-iPr$_2$)$_2$}] (**7**).

EXPERIMENTAL SECTION

All experiments were performed in evacuated tubes, using standard Schlenk-tube or glovebox techniques, with rigorous exclusion of traces of moisture and air. After drying over KOH, THF and DME were purified by distillation from sodium/benzophenone ketyl and hexane, benzene, and toluene by distillation from sodium/triglyme benzophenone ketyl prior to use. C$_6$D$_6$ was dried with sodium/benzophenone ketyl and condensed under vacuum prior to use. [tBuC(NHC$_6$H$_3$-2,6-iPr$_2$)(NC$_6$H$_3$-2,6-iPr$_2$)],[26] [2,6-iPr$_2$C$_6$H$_3$N=C(H)C(H)=NC$_6$H$_3$-2,6-iPr$_2$] (DAD),[17] and [(Me$_3$SiCH$_2$)$_3$Yb(THF)$_2$][27] were prepared according to literature procedures. PhSiH$_3$ was purchased from Aldrich, stored over CaH$_2$, and condensed under vacuum prior to use. CuCl and (PhCH$_2$S)$_2$ were purchased from Aldrich and were used without any additional purification. NMR spectra were recorded on a Bruker Avance-II 400 MHz spectrometer. Chemical shifts for ^{1}H and ^{13}C spectra were referenced internally using the residual solvent resonances and are reported relative to TMS. The ^{171}Yb chemical shift was referenced internally and is reported relative to (C$_5$Me$_5$)$_2$Yb-(THF)$_2$ (1 M solution in THF). Lanthanide metal analysis was carried out by complexometric titration. The C, H, N elemental analysis was carried out in the microanalytical laboratory of the IOMC.

Synthesis of [{tBuC(NC$_6$H$_3$-2,6-iPr$_2$)$_2$}Yb(μ-Cl)]$_2$ (2). A suspension of CuCl (0.046 g, 0.466 mmol) in 5 mL of toluene was added to a solution of **1** (0.277 g, 0.233 mmol) in toluene (25 mL) at −60 °C with stirring. The reaction mixture was warmed to room temperature and was stirred for an additional 12 h. The Cu precipitate was removed by filtration. Slow concentration of a toluene solution at room temperature afforded crystals of **2** (0.246 g, 84% yield). ^{1}H NMR (400 MHz, C$_6$D$_6$, 293 K): 1.22−1.37 (complex m, 48H, CH_3 iPr), 1.44 (s, 18H, CH_3 tBu), 3.19−3.45 (complex m, 8H, CH iPr), 6.94 (d, $^3J_{HH}$ = 8.1 Hz, 2H, CH Ar), 7.01−7.11 (complex m, 10H, CH Ar), 7.23 (d, $^3J_{HH}$ = 7.4 Hz, 2H, CH Ar) ppm. ^{13}C{^{1}H} NMR (100 MHz, C$_6$D$_6$, 293 K): 20.0 (br s, CH_3 iPr), 21.2 (br s, CH_3 iPr), 23.4 (br s, CH_3 iPr), 25.7 (s, CH_3 iPr), 28.3 (br s, CH iPr), 29.7 (s, CH iPr), 31.2 (s, CH_3 tBu), 41.8 (s, CMe_3, with ^{171}Yb satellites $^3J_{YbC}$ = 25.7 Hz), 123.0 (br s, CH Ar), 123.8 (br s, CH Ar), 124.7 (br s, CH Ar), 142.5 (br s, C Ar), 143.4 (br s, C Ar), 144.3 (br s, C Ar), 147.6 (br s, C Ar), 171.5 (s, with ^{171}Yb satellites $^2J_{YbC}$ = 50.1 Hz, NCN) ppm. Anal. Calcd for C$_{58}$H$_{86}$Cl$_2$N$_4$Yb$_2$ (1256.34 g/mol): C, 55.45; H, 6.90; N, 4.46; Yb, 27.55. Found: C, 55.50; H, 7.00; N, 4.36; Yb, 27.42.

Synthesis of [{tBuC(NC$_6$H$_3$-2,6-iPr$_2$)$_2$}Yb(μ-SCH$_2$Ph)]$_2$ (3). A toluene solution (5 mL) of (PhCH$_2$S)$_2$ (0.040 g, 0.163 mmol) was added to a solution of **1** (0.194 g, 0.163 mmol) in toluene (25 mL) at

dx.doi.org/10.1021/om400015k | Organometallics 2013, 32, 1507−1516

Table 1. Main Crystallographic Data and Structure Refinement Details for 3−7

	3	4	5	6	7
formula	$C_{72}H_{100}N_4S_2Yb_2{\cdot}C_7H_8$)	$C_{86}H_{114}N_4S_4Yb_2$	($C_{52}H_{72}N_4Yb$), ($C_{37}H_{63}N_2O_4Yb$)$\cdot^1/_6C_6H_6\cdot^1/_6C_6H_{14}\cdot^1/_6C_4H_8O$	$C_{41}H_{73}N_2OSi_2Yb$	$C_{70}H_{97}N_4PYb_2$
M_r	1523.89	1678.13	1738.51	839.23	1371.57
cryst size, mm^3	0.2 × 0.2 × 0.1	0.2 × 0.2 × 0.04	0.17 × 0.16 × 0.03	0.35 × 0.30 × 0.15	0.2 × 0.1 × 0.05
T, K	100(2)	100(2)	100(2)	100(2)	100(2)
cryst syst	triclinic	monoclinic	triclinic	monoclinic	monoclinic
space group	$P\bar{1}$	$P2_1/n$	$P\bar{1}$	$P2_1/c$	$C2/c$
a, Å	12.7391(3)	15.4161(4)	20.671(2)	11.9708(7)	15.2958(2)
b, Å	14.3319(3)	17.4607(4)	26.709(3)	13.2488(7)	21.1987(3)
c, Å	21.0538(6)	15.9777(4)	29.791(3)	27.7865(16)	19.8807(3)
α, deg	75.308(2)	90	111.023(2)	90	90
β, deg	82.800(2)	114.938(3)	106.486(3)	93.5430(10)	90.602(1)
γ, deg	89.461(2)	90	97.723(3)	90	90
cell vol, $Å^3$	3687.90(17)	3899.81(19)	14200(3)	4398.5(4)	6446.00(16)
Z	2	2	6	4	4
D_{calcd}, g/cm^3	1.372	1.429	1.220	1.267	1.413
μ, mm^{-1}	2.620	2.537	2.011	2.211	2.951
F_{000}	1564	1724	5430	1756	2800
2θ range, deg	2.94−26.00	3.04−30.00	1.34−25.97	2.13−26.00	3.18−30.00
index ranges	$-15 \le h \le 15$	$-21 \le h \le 21$	$-23 \le h \le 25$	$-14 \le h \le 14$	$-21 \le h \le 21$
	$-17 \le k \le 17$	$-24 \le k \le 24$	$-28 \le k \le 32$	$-16 \le k \le 16$	$-29 \le k \le 29$
	$-25 \le l \le 25$	$-22 \le l \le 22$	$-36 \le l \le 31$	$-34 \le l \le 34$	$-27 \le l \le 27$
no. of rflns collected	55204	79002	84342	37006	65032
no. of indep rflns	14080	11337	54635	8623	9396
R_{int}	0.0722	0.1436	0.2078	0.0307	0.0958
completeness to θ, %	97.1	99.6	98.1	99.8	99.9
no. of data/restraints/params	14080/160/796	11337/0/444	54635/1083/2530	8623/26/496	9396/0/360
GOF	1.039	0.945	0.823	1.058	1.037
final R indices ($I > 2\sigma(I)$)	R1 = 0.0575	R1 = 0.0500	R1 = 0.1105	R1 = 0.0294	R1 = 0.0409
	wR2 = 0.1216	wR2 = 0.0667	wR2 = 0.1754	wR2 = 0.0672	wR2 = 0.0572
R indices (all data)	R1 = 0.0759	R1 = 0.0910	R1 = 0.3462	R1 = 0.0384	R1 = 0.0682
	wR2 = 0.1281	wR2 = 0.0742	wR2 = 0.2314	wR2 = 0.0702	wR2 = 0.0613
largest diff peak/hole, e $Å^3$	4.079/−1.503	1.695/−1.847	1.552/−1.523	1.499/−0.855	1.087/−1.142

−60 °C. The reaction mixture was stirred for 2 h at −60 °C and then was warmed to room temperature and stirred for an additional 2 h. After removal of toluene, the solid residue was dissolved in hexane. Slow concentration of the resulting solution at room temperature afforded red-purple crystals of **3** (0.211 g, 90% yield). ^{1}H NMR (400 MHz, C_6D_6, 293 K): 0.51 (br s, 12H, CH_3 *i*Pr), 0.89 (s, 18H, CH_3 *t*Bu), 1.21−1.34 (complex m, 36H, CH_3 *i*Pr), 3.04−3.54 (complex m, 12H, C*H* *i*Pr and SCH_2), 6.90−7.05 (complex m, 22H, C*H* Ar) ppm. $^{13}C\{^1H\}$ NMR (100 MHz, C_6D_6, 293 K): 21.5 (br s, CH_3 *i*Pr), 21.6 (br s, CH_3 *i*Pr), 25.1 (br s, CH_3 *i*Pr), 26.4 (br s, CH_3 *i*Pr), 28.3 (br s, *C*H *i*Pr), 28.4 (br s, *C*H *i*Pr), 30.2 (s, CH_3 *t*Bu), 34.6 (s, SCH_2), 45.7 (s, with ^{171}Yb satellites $^3J_{YbC}$ = 45.1 Hz, *C*Me_3), 122.5 (s, *C*H Ar), 122.8 (s, *C*H Ar), 125.8 (s, *C*H Ar), 128.2 (s, *C*H Ar), 128.4 (s, *C*H Ar), 129.0 (s, *C*H Ar), 140.1 (br s, *C* Ar), 140.5 (br s, *C* Ar), 141.7 (s, *C* Ar), 145.8 (s, *C* Ar), 173.9 (s, with ^{171}Yb satellites $^2J_{YbC}$ = 22.5 Hz, NCN) ppm. Anal. Calcd for $C_{72}H_{100}N_4S_2Yb_2$ (1431.83 g/mol): C, 60.40; H, 7.04; N, 3.91; Yb, 24.17. Found: C, 59.73; H, 6.89; N, 3.86; Yb, 24.12.

Synthesis of [{*t*BuC(NC$_6$H$_3$-2,6-*i*Pr$_2$)$_2$}Yb(*μ*-SCH$_2$Ph)$_2$]$_2$ (4). *Method A.* A toluene solution (5 mL) of $(PhCH_2S)_2$ (0.102 g, 0.413 mmol) was added to a solution of **1** (0.245 g, 0.206 mmol) in toluene (25 mL) at −60 °C. The reaction mixture was stirred for 2 h at −60 °C and then warmed to room temperature and stirred for an additional 2 h. Slow concentration of the resulting solution at room temperature afforded bright yellow crystals of **4** (0.319 g, 92% yield). Anal. Calcd for $C_{86}H_{114}N_4S_4Yb_2$ (1678.22 g/mol): C, 61.55; H, 6.85; N, 3.34; Yb, 20.62. Found: C, 61.68; H, 6.97; N, 3.14; Yb, 20.51.

Method B. A toluene solution (5 mL) of $(PhCH_2S)_2$ (0.031 g, 0.124 mmol) was added to a solution of **3** (0.178 g, 0.124 mmol) in toluene (10 mL) at room temperature. The reaction mixture was stirred for 3 h. Slow concentration of the resulting solution at room temperature afforded bright yellow crystals of **4** (0.159 g, 76% yield).

Reaction of 1 with [2,6-*i*Pr$_2$C$_6$H$_3$NC(H)═C(H)NC$_6$H$_3$-2,6-*i*Pr$_2$]. Synthesis of [{*t*BuC(NC$_6$H$_3$-2,6-*i*Pr$_2$)$_2$}Yb(DME)$_2$]$^+$[{2,6-*i*Pr$_2$C$_6$H$_3$NC(H)═C(H)NC$_6$H$_3$-2,6-*i*Pr$_2$}$_2$Yb]$^-$ (5). A solution of DAD (0.167 g, 0.443 mmol) in toluene (5 mL) was added to a solution of **1** (0.263 g, 0.221 mmol) in toluene (25 mL) at room temperature. The reaction mixture was heated to 50 °C and was stirred for 12 h. The solvent was removed under vacuum, and the solid residue was treated with DME (5 mL). The resultant solution was warmed to 50 °C for 1 h, the solvent was removed under vacuum, and the solid residue was dissolved in a THF/benzene/hexane (1/1/1) mixture (15 mL). Slow concentration of the resulting solution at room temperature afforded **5** (0.086 g, 23% yield). Anal. Calcd for $C_{89}H_{135}N_6O_4Yb_2$ (1697.63 g/mol): C, 62.91; H, 8.01; N, 4.95; Yb, 20.37. Found: C, 63.29; H, 8.53; N, 4.71; Yb, 19.94.

Synthesis of [{*t*BuC(NC$_6$H$_3$-2,6-*i*Pr$_2$)$_2$}Yb(CH$_2$SiMe$_3$)$_2$(THF)] (6). A THF solution (10 mL) of [*t*BuC(NHC$_6$H$_3$-2,6-*i*Pr$_2$)(NC$_6$H$_3$-2,6-*i*Pr$_2$)] (0.498 g, 1.183 mmol) was added to a solution of $(Me_3SiCH_2)_3Yb(THF)_2$ (0.685 g, 1.183 mmol) in THF (10 mL) at 0 °C. The reaction mixture was stirred for 2 h and then was warmed to room temperature and stirred for 12 h. THF was removed under vacuum, and the solid residue was dissolved in hexane (25 mL). Slow concentration of the resulting solution at room temperature afforded

dx.doi.org/10.1021/om400015k | *Organometallics* 2013, 32, 1507−1516

orange-yellow crystals of **6** (0.754 g, 76% yield). Anal. Calcd for $C_{41}H_{73}N_2OSi_2Yb$ (839.26 g/mol): C, 58.68; H, 8.77; N, 3.34; Yb, 20.62. Found: C, 59.29; H, 8.93; N, 3.27; Yb, 20.44.

Reaction of 6 with $PhSiH_3$ (1:2 Molar Ratio). $PhSiH_3$ (0.109 g, 1.003 mmol) was added to a solution of **6** (0.428 g, 0.501 mmol) in toluene (20 mL) at 0 °C. The reaction mixture was stirred for 2 h and then was warmed to room temperature and stirred for 12 h. Toluene was removed under vacuum, and the solid residue was washed with hexane (10 mL). Further recrystallization of the solid residue from toluene by slow concentration at 50 °C resulted in formation of black crystals of **1** (0.250 g, 84%). ^{1}H NMR (400 MHz, C_6D_6, 293 K): 0.91 (s, 18H, CH_3 *t*Bu), 1.22−1.37 (complex m, 48H, CH_3 *i*Pr), 3.24−3.55 (complex m, 8H, C*H* *i*Pr), 6.93−7.10 (complex m, 12H, C*H* Ar), 7.74 (s, 2H, with ^{171}Yb satellites, $^1J_{YbH}$ = 460 Hz) ppm. Anal. Calcd for $C_{58}H_{88}N_4Yb_2$ (1187.45 g mol^{-1}): C, 58.67; H, 7.47; N, 4.72; Yb, 29.15. Found: C, 59.05; H, 7.72; N, 4.46; Yb, 28.95.

Reaction of 6 with $PhSiH_3$ (1:1 Molar Ratio). $PhSiH_3$ (0.065 g, 0.599 mmol) was added to a solution of **6** (0.503 g, 0.599 mmol) in toluene (20 mL) at 0 °C. The reaction mixture was stirred for 2 h and then was warmed to room temperature and stirred for 12 h. Toluene was removed under vacuum, and the solid residue was extracted with hexane (15 mL). The solution was separated from the solid residue by decantation. Slow concentration of the resulting hexane solution at room temperature afforded orange-yellow crystals of **6** (0.176 g, 35% yield). Complex **6** was identified by microanalysis. Recrystallization of the solid residue from toluene by slow concentration at 50 °C afforded **1** (0.142 g, 40% yield). Complex **1** was identified by its spectral characteristics and microanalysis.

Synthesis of [{*t*BuC(NC$_6$H$_3$-2,6-*i*Pr$_2$)$_2$}Yb(μ-H)(μ-PPh$_2$)Yb-{*t*BuC(NC$_6$H$_3$-2,6-*i*Pr$_2$)$_2$}] (7). A solution of Ph_2PH (0.100 g, 0.542 mmol) in toluene (5 mL) was slowly added to a solution of **1** (0.322 g, 0.271 mmol) in toluene (25 mL) at 0 °C. The reaction mixture was stirred at this temperature for 1 h and then warmed to room temperature and stirred for 1 h. Recrystallization of the solid residue from a toluene/hexane (1/1) mixture by slow concentration at room temperature resulted in the formation of **7** (0.180 g, 82% yield). ^{1}H NMR (400 MHz, C_6D_6, 293 K): 1.21−1.34 (complex m, 48H, CH_3 *i*Pr), 1.50 (s, 18H, CH_3 *t*Bu), 3.23−3.36 (complex m, 8H, C*H* *i*Pr), 6.57 (t, $^3J_{HH}$ = 7.6 Hz, 2H, *p*-C*H* PPh), 6.65 (t, $^3J_{HH}$ = 7.6 Hz, 4H, *o*-C*H* PPh), 6.97 (m, 4H, C*H* Ar), 7.05 (t, $^3J_{HH}$ = 7.8 Hz, 4H, *m*-C*H* PPh), 7.14 (m, 8H, C*H* Ar), 8.25 (d, $^2J_{PH}$ = 52 Hz, with ^{171}Yb satellites $^1J_{YbH}$ = 486 Hz, 1H, Yb*H*) ppm. ^{13}C{^{1}H} NMR (100 MHz, C_6D_6, 293 K): 22.4 (s, CH_3 *i*Pr), 23.4 (s, CH_3 *i*Pr), 25.3 (s, CH_3 *i*Pr), 27.8 (s, CH_3 *i*Pr), 28.7 (s, CH *i*Pr), 29.1 (s, CH *i*Pr), 31.2 (s, CH_3 *t*Bu), 41.9 (s, CMe_3), 118.1 (s, *p*-CH PPh), 122.8 (s, CH Ar), 124.1 (s, CH Ar), 124.3 (s, CH Ar), 124.6 (s, CH Ar), 128.2 (s, *m*-CH PPh) 132.1 (d, $^1J_{PC}$ = 14.9 Hz, *o*-CH PPh), 141.8 (d, $^1J_{PC}$ = 6.6 Hz, *ipso*-C PPh), 142.3 (s, C Ar), 142.4 (s, C Ar), 143.5 (s, C Ar), 170.4 (s, NCN) ppm. ^{31}P{^{1}H} NMR (161.98 MHz, C_6D_6, 293 K): 30.9 (s, with ^{171}Yb satellites $^1J_{YbP}$ = 810 Hz) ppm. ^{171}Yb{^{1}H} NMR (69.8 MHz, C_6D_6, 293 K): 1149 (d, $^1J_{YbP}$ = 810 Hz) ppm. The 2D Yb−H *g*-HSQC NMR spectrum was set with the hsqcetgp pulse program, delay D1 = 1.5 s, cnst2 = 200, GPZ2 = 14%: {6.69; 7.57; 8.18; 8.79; 9.40}{1143.2}, {7.10; 7.70; 8.31; 8.92; 9.53}{1154.8} (see the Supporting Information). Anal. Calcd for $C_{70}H_{97}N_4PYb_2$ (1371.63 g/mol): C, 61.30; H, 7.13; N, 4.08; Yb, 25.23. Found: C, 61.37; H, 7.28; N, 4.02; Yb, 25.18.

X-ray Crystallography. The X-ray data were collected on a Smart Apex diffractometer (for **5** and **6**, graphite-monochromated Mo Kα radiation, ω-scan technique, λ = 0.71073 Å, T = 100(2) K) and a Agilent Xcalibur E diffractometer (for **3**, **4**, and **7**, graphite-monochromated Mo Kα radiation, ω-scan technique, λ = 0.71073 Å, T = 100(2) K). The structures were solved by direct methods and were refined on F^2 using the SHELXTL[28] (**5** and **6**) and CrysAlis Pro[29] (**3**, **4**, and **7**) packages. All non-hydrogen atoms were found from Fourier syntheses of electron density and were refined anisotropically. $H^{C30,C34}$ in **6** and H1 in **7** were also found from Fourier syntheses of electron density but were refined isotropically. All other hydrogen atoms were placed in calculated positions and were refined in the riding model. SADABS[30] (**5** and **6**) and ABSPACK (CrysAlis Pro)[29] (**3**, **4**, and **7**) were used to perform area-detector scaling and absorption corrections. Crystallographic data and collection and refinement details are shown in Table 1, and the corresponding CIF files are available as Supporting Information. CCDC-918719 (**3**), CCDC-918720 (**4**), CCDC-918721 (**5**), CCDC-918722 (**6**), and CCDC-918723 (**7**) also contain supplementary crystallographic data for this paper. These data can be obtained free of charge from The Cambridge Crystallographic Data Centre via ccdc.cam.ac.uk/products/csd/request/.

■ ASSOCIATED CONTENT

Ⓢ Supporting Information

Figures giving NMR spectra and CIF files giving crystallographic data for the structures determined in this paper. This material is available free of charge via the Internet at http://pubs.acs.org.

■ AUTHOR INFORMATION

Corresponding Author

*E-mail: trif@iomc.ras.ru.

Notes

The authors declare no competing financial interest.

■ ACKNOWLEDGMENTS

This work was supported by the Russian Foundation for Basic Research (Grant No 12-03-31865) and Ministry of Science and Innovations of N. Novgorod region (Grant No 11-03-97030-p), Grant of President of Russian Federation for young scientists (Grant No MK-4908.2012.3, DML), The Ministry of education and science of Russian Federation (project No. 8445).

■ REFERENCES

(1) (a) Werkema, E. L.; Messines, E.; Perrin, L.; Maron, L.; Eisenstein, O.; Andersen, R. A. *J. Am. Chem. Soc.* **2005**, *127*, 7781−7795. (b) Maron, L.; Werkema, E. L.; Perrin, L.; Eisenstein, O.; Andersen, R. A. *J. Am. Chem. Soc.* **2005**, *127*, 279−292.

(2) For selected reviews on rare-earth hydrido complexes, see: (a) Nishiura, M.; Hou, Z. *Nat. Chem.* **2010**, *2*, 257−268. (b) Konkol, M.; Okuda, J. *Coord. Chem. Rev.* **2008**, *252*, 1577−1591. (c) Trifonov, A. A. *Russ. Chem. Rev.* **2007**, *76*, 1051−1072. (d) Hou, Z.; Nishiura, M.; Shima, T. *Eur. J. Inorg. Chem.* **2007**, 2535−2545. (e) Hou, Z. *Bull. Chem. Soc. Jpn.* **2003**, *76*, 2253−2266. (f) Okuda, J. *Dalton Trans.* **2003**, 2367−2378. (g) Ephritikhine, M. *Chem. Rev.* **1997**, *97*, 2193−2242.

(3) (a) Evans, W. J.; Meadows, J. H.; Wayda, A. L. *J. Am. Chem. Soc.* **1982**, *104*, 2015−2017. (b) Evans, W. J.; Meadows, J. H.; Hanusa, T. P. *J. Am. Chem. Soc.* **1984**, *106*, 4454−4460. (c) Evans, W. J.; Sollberger, M. S.; Khan, S. I.; Bau, R. *J. Am. Chem. Soc.* **1988**, *110*, 439−446.

(4) (a) Ferrence, G. M.; McDonald, R.; Takats, J. *Angew. Chem., Int. Ed.* **1999**, *38*, 2233−2237. (b) Ruspic, C.; Spielman, J.; Harder, S. *Inorg. Chem.* **2007**, *46*, 5320−5326. (c) Basalov, I. V.; Lyubov, D. M.; Fukin, G. K.; Shavyrin, A. S.; Trifonov, A. A. *Angew. Chem., Int. Ed.* **2012**, *52*, 3444−3447.

(5) Takenaka, Y.; Hou, Z. *Organometallics* **2009**, *28*, 5196−5203.

(6) Evans, W. J.; Hozbor, M. A. *J. Organomet. Chem.* **1987**, *326*, 299−306.

(7) Nief, F.; Ricard, L. *J. Chem. Soc., Chem. Commun.* **1994**, 2723−2724.

(8) Edelmann, F. T. *Adv. Organomet. Chem.* **2008**, *57*, 183−352.

(9) (a) Yao, S.; Chan, H.-S.; Lam, C.-K.; Lee, H. K. *Inorg. Chem.* **2009**, *48*, 9936−9946. (b) Wang, J.; Yao, Y.; Zhang, Y.; Shen, Q. *Inorg. Chem.* **2009**, *48*, 744−751. (c) Luo, Y.; Yao, Y.; Shen, Q.; Sun, J.; Weng, L. *J. Organomet. Chem.* **2002**, *662*, 144−149.

(10) Heitmann, D.; Jones, C.; Junk, P. C.; Lippert, K.-A.; Stasch, A. *Dalton Trans.* **2007**, 187−189.
(11) Shannon, R. D. *Acta Crystallogr.* **1976**, *A32*, 751−767.
(12) Trifonov, A. A. *Eur. J. Inorg. Chem.* **2007**, 3151−3167.
(13) Allen, F. A.; Konnard, O.; Watson, D. G.; Brammer, L.; Orpen, G.; Taylor, R. *J. Chem. Soc., Perkin Trans.* **1987**, 1−19.
(14) Panda, T. K.; Kaneko, H.; Pal, K.; Tsurugi, H.; Mashima, K. *Organometallics* **2010**, *29*, 2610−2615.
(15) Trifonov, A. A.; Borovkov, I. A.; Fedorova, E. A.; Fukin, G. K.; Larionova, J.; Druzhkov, N. O.; Cherkasov, V. K. *Chem. Eur. J.* **2007**, *13*, 4981−4987.
(16) For Yb(III)−N bonds see: (a) Schulz, M.; Boncella, J. M.; Berg, D. J.; Tilley, T. D.; Andersen, R. A. *Organometallics* **2002**, *21*, 460−472. (b) Zhou, X.; Huang, Z.; Cai, R.; Zhang, L.-B.; Zhang, L.-X; Huang, X. *Organometallics* **1999**, *18*, 4128−4133.
(17) Laine, T. V.; Klinga, M.; Maaninen, A.; Aitola, E.; Leskelä, M. *Acta Chem. Scand.* **1999**, *53*, 968−973.
(18) (a) Lyubov, D. M.; Döring, C.; Fukin, G. K.; Cherkasov, A. V.; Shavyrin, A. V.; Kempe, R.; Trifonov, A. A. *Organometallics* **2008**, *27*, 2905−2907. (b) Lyubov, D. M.; Döring, C.; Ketkov, S. Yu.; Kempe, R.; Trifonov, A. A. *Chem. Eur. J.* **2011**, *17*, 3824−3826.
(19) (a) Nishiura, M.; Baldamus, J.; Shima, T.; Mori, K.; Hou, Z. *Chem. Eur. J.* **2011**, *17*, 5033−5044. (b) Li, S.; Miao, W.; Tang, T.; Cui, D.; Chen, X.; Jing, X. *J. Organomet. Chem.* **2007**, *692*, 4943−4952. (c) Cheng, J.; Saliu, K.; Kiel, G. Y.; Ferguson, M. J.; McDonald, R.; Takats, J. *Angew. Chem., Int. Ed.* **2008**, *47*, 4910−4913.
(20) For other examples of intramolecular metal reduction by hydrido ligands see: (a) Nöth, H.; Schmidt, M. *Organometallics* **1995**, *14*, 4601−4610. (b) Fischer, J. M.; Piers, W. E.; Pearce-Batchilder, S. D.; Zaworotko, M. J. *J. Am. Chem. Soc.* **1996**, *118*, 283−284. (c) Ma, K.; Piers, W. E.; Gao, Y.; Parvez, M. *J. Am. Chem. Soc.* **2004**, *126*, 5668−5669.
(21) Cheng, J.; Saliu, K.; Ferguson, M. J.; McDonald, R.; Takats, J. *J. Organomet. Chem.* **2010**, *695*, 2696−2702.
(22) For other examples of σ-bond metathesis between P−H and Ln−X (X = C, H) bonds see: (a) Evans, W. J.; Bloom, I.; Hunter, W. E.; Atwood, J. L. *Organometallics* **1983**, *2*, 709−714. (b) Zhang, W.-X.; Nishiura, M.; Mashiko, T.; Hou, Z. *Chem. Eur. J.* **2008**, *14*, 2167−2179. (c) Nolan, S. P.; Stern, D.; Marks, T. J. *J. Am. Chem. Soc.* **1989**, *111*, 7844−7853.
(23) (a) Tardif, O.; Hou, Z.; Nishiura, M.; Koizumi, T.; Wakatsuki, Y. *Organometallics* **2001**, *20*, 4565−4573. (b) Rabe, G. W.; Riede, J.; Schier, A. *Inorg. Chem.* **1996**, *35*, 40−45.
(24) For $^{31}P\{^{1}H\}$ chemical shifts and $^{31}P-^{171}Yb$ coupling constants in related Yb(II) complexes see the following. (a) $Yb[PPh_2]_2(THF)_4$: δ −3.0 ppm, $^{1}J_{YbP}$ = 840 Hz. Rabe, G. W.; Yap, J. G. P. A.; Meingold, A. L. *Inorg. Chem.* **1995**, *34*, 4521−4522. (b) $Yb[(\mu\text{-}PtBu_2)_2Li(THF)]_2$: δ 62.5 ppm, $^{1}J_{YbP}$ = 873 Hz. Rabe, G. W.; Riede, J.; Schier, A. *Inorg. Chem.* **1996**, *35*, 40−45.
(25) For $^{171}Yb\{^{1}H\}$ chemical shifts in related Yb(II) complexes see the following: **1**, δ 1536 ppm;[4c] $[(Tp^{tBu,Me})YbH]_2$, δ 772 ppm.[4a] For $[\{([Me_3Si]_2CH)(C_6H_4\text{-}2\text{-}CH_2NMe_2)P\}_2Yb]$, δ 864 ppm, see: Izod, K.; O'Shaughnessy, P.; Sheffield, J. M.; Clegg, W.; Liddle, S. T. *Inorg. Chem.* **2000**, *39*, 4741−4748.
(26) Xia, A.; El-Kaderi, H. M.; Heeg, M. J.; Winter, C. H. *J. Organomet. Chem.* **2003**, *682*, 224−232.
(27) (a) Atwood, J. L.; Hunter, W. E.; Rogers, R. D.; Holton, J.; McMeeking, J.; Pearce, R.; Lappert, M. F. *J. Chem. Soc., Chem. Commun.* **1978**, 140−142. (b) Lappert, M. F.; Pearce, R. J. *J. Chem. Soc., Chem. Commun.* **1973**, 126−127. (c) Schumann, H.; Freckmann, D. M. M.; Dechert, S. *Z. Anorg. Allg. Chem.* **2002**, *628*, 2422−2426.
(28) Sheldrick, G. M. *SHELXTL v.6.12, Structure Determination Software Suite*; Bruker AXS, Madison, WI, 2000.
(29) *CrysAlis Pro*; Agilent Technologies Ltd, Yarnton, England, 2011.
(30) Sheldrick, G. M. *SADABS v.2.01, Bruker/Siemens Area Detector Absorption Correction Program*; Bruker AXS, Madison, WI, 1998.